doi.org/10.36721/PJPS.2025.38.5.REG.13901.1

In-vitro microbiological evaluation of gemifloxacin derivatives: Synthesis, vibrational spectroscopy, molecular docking and DFT studies

Sana Shamim[1]*, Rabya Munawar[1], Majid Ali[2], Nasir Shahzad[2], Sonia Khan[3], Irshad Begum[4] and Safia Khan[4]

[1]Department of Pharmaceutical Chemistry, Dow College of Pharmacy, Faculty of Pharmaceutical Sciences, Dow University of Health Sciences, Ojha Campus Karachi, Pakistan.
[2]Department of Higher Education, Khyber Pakhtoon Khwa, Pakistan.
[3]Al-Tibri Medical College, Karachi, Pakistan.
[4]Department of Chemistry, University of Karachi, Pakistan.

Abstract: Herein, to address the challenges associated with microbial resistance against antibiotics, three new gemifloxacin derivatives (G-D08, G-D09 and G-D10), have been synthesized using conventional esterification (Fischer) and amide approach (C-3 and C-7 modified) in efficient yields. UV-Vis, FT-IR, ^{1}HNMR, and Mass spectroscopy for characterization while DFT studies for computational conformational stability. In-silico pharmacokinetics (Swiss ADME, Bio transformers) and toxicological properties (T.E.S.T software) evaluated that all derivatives followed Lipinski's criterion and exhibits no vital organ toxicity. Microbiological evaluation in reciprocation towards designated strains of Gram +ve and Gram -ve bacteria, and fungi demonstrated potent actuation towards *K. pneumonia, Candida albicans* and *Citrobacter freundii* in comparison to gemifloxacin, surpassing antibacterial and antifungal responsiveness, reinforced by B3LYP/6–311 G level of theory. Energy gaps (HOMO-LUMO) of derivative G-D09 and G-D10 is 1.72 eV determinant as cognizant. Molecular docking approach was also applied through MOE software against *K. pneumonia* (PDB ID: 6k63)*, C. freundii* (PDB ID: 3JWB) and *C. albicans* (PDB ID: 1AI9) ranging between -6.05 and -7.79 kcal/ mol, authenticating their higher antibacterial response towards *Klebsiella pneumoniae* among all compounds and G-D10 as potent antifungal agent.

Keywords: Gemifloxacin, derivatives, antifungal, ADME, DFT, molecular docking.

Submitted on 19-12-2024 – Revised on 26-02-2025– Accepted on 11-04-2025

INTRODUCTION

The world is currently dealing with a hype in infection treatment failure because of acquired drug resistance towards antibiotics, giving rise to severity in disease condition and morbidity in recent years. (Akunuri, Veerareddy *et al*., 2021) Irregular and extensive use of antibiotic has caused harmful bacteria to adapt several mechanisms leading to change their intrinsic characteristics, thus leading to antibiotics response failure either by extruding a variety of medications or altering genetic expressions that encode drug efflux through pumping. These concerns lead to higher complexity in managing protocols in wellness programs, which affects Gram -ve, and Gram +ve infections, leading to high global morbidity and mortality. (Dadgostar P 2019) To combat this, researchers are trying to develop new, stronger and efficient antibiotics to overcome resistant issues. (Mlynarczyk, Kowalewski *et al.,* 2022).

Quinolones, pioneer members of anti-microbial drugs, revolutionized with exploration of 6-Fl analogs, allowing it to evolve as broader spectrum antibiotics. This intimates adaptations in structural modification to escalate potency and microbial resistance development. As these antimicrobial agents also delineated anomalous responses such as anti-tumor (Yadav, Talwar 2019), anti-tubercular (Fan, Wu *et al*., 2018), anti-HIV (Wang, Xu *et al*., 2019), anti-malarial (Balogun, Omoboyowa *et al*., 2020) and anti-Alzheimer activities. (Luo, Lv *et al*., 2020).

Structure-activity relationship (SAR) investigations of fluoroquinolones have shown that presence of basic groups at C-3 and C-7 positions of quinolone ring, with functional groups substitution exhibits significant impact on their antibacterial response, spectrum, and safety correlated with high lipophilicity. (Shamim, Naseem *et al.,* 2024; Stapleton, Ansari *et al*., 2023; Ezelarab, Abbas *et al*., 2018). Preferably, acidic groups present at this position are going to enhance/control the receptor binding affinities of drug molecules suggested and evident by various studies. (El-Emam, El-Baz *et al*., 2023; Zhao, Zhang *et al*., 2023) Co-relating with the acidic functionality controls pka of hydrogen group at this position representing carboxylic proton in parent quinolone molecule. Some research groups have worked at same position by modifying by either an anionic, amides or esters groups, resulting in enhanced potency and efficacy against resistant species.

**Corresponding author:* e-mail: sana.shamim@duhs.edu.pk

While, analogues with modified carboxylic acid at position C-3 of a fluoroquinolone do not significantly affcet antibacterial response in vivo, with exception of groups that are changed back to carboxylic acid or behaving as pro-drug (Jia, Zhao 2021). Substituted 3-carboxylic acid with acidic groups, such as phosphoric acid , acetic acid, hydroxamic acid, sulfonic acid (Sharma, Das *et al.,* 2022), or a molecule that mimics carboxylic acid exhibits significantly reduced antibacterial activity as they alter the pka values and dissociation ability of the analogs. (Ezelarab, Abbas *et al*., 2018). In light of these studies, our research lab has previously worked on synthesis of several quinolone derivatives, by carrying out synthesis of gatifloxacin derivatives (C-7 alteration). (Zaharani, Khaligh *et al.,*2021), reveals that addition of an acetyl or benzoyl group causes reduced antimicrobial response, whereas modification of COOH group attenuate therapeutic profile as in case of levofloxacin (C-3 position) that were more effective against bacteria than parent molecule. (Zhao, Zhang *et al*., 2023)

Therefore, as part of our ongoing research, we alter Gemifloxacin (GMFX) fig. 1, fluoronaphthyridone quinolone with a 7-pyrrolidone substituent a potent member of fluoroquinolone class responsive towards both Gram +ve and Gram -ve organisms including respiratory tract infection pathogens. (El-Emam, El-Baz *et al*., 2023; Tangwangvivat, Chaiyawong *et al*., 2022; Sakr, El Kafrawy *et al*., 2022). Gemifloxacin analogues were synthesized by conventional fischer esterification and nucleophilic reaction method. (Zaharani, Khaligh *et al*., 2017) The derivatives were characterized using variety of spectroscopic techniques, (Mass, ^{1}HNMR, FTIR and UV-visible). Additionally, it would be intriguing to look into the biological effects that this new ligand and its derivatives have on some gram-positive and gram-negative organisms. Moreover, molecular docking studies applied to support these in vitro microbiological results (Hassan, Allam *et al*., 2020) as it apprehends molecular interaction on basis of binding affinities. (Gökalp, Dede *et al*., 2020).

MATERIALS AND METHODS

Chemicals and reagents were of analytical grades (≥ 99%)) Sigma-Aldrich, Darmstadt, German, GMFX (Genix Pharma, Karachi as gift sample). Dynalon SMP10 (digital thermometer) was used for melting points. For the reaction completion and purity determination TLC system (CH_3OH /NH_3 /$C_4H_9O_6$ (0.7: 1.8:5.5)) was developed, using (Silica gel 60 aluminum-backed plates 0.063–0.200 mm), observed under UV light (254 nm). Characterized by FT-IR (Shimadzu 470), ^{1}HNMR (Bruker XWIN NMR, $CDCl_3$; DMSO as solvent) and EIMS spectra (MAT 312 mass spectrometer; Jeol MS instrument (range 50–800)), respectively.

Synthesis of derivative G-D08

In this work, we synthesized a derivative of GMFX by esterification at 3-carboxylic acid after reacting with phenol (resorcinol) applying Fischer esterification in equi-molar ratio. Sulphuric acid (conc.), used as catalyst to generate the ester following an acid-catalyzed esterification reaction (Scheme 1).

(E)-3-hydroxyphenyl 7-(3-(aminomethyl)-4-(methoxyimino) pyrrolidin-1-yl)-1-cyclopropyl-6-fluoro-4-hydroxy-1, 4-dihydro-1, 8-naphthyridine-3-carboxylate (G-D08)

483.49, 154°C, Brown, DMSO, methanol, Chloroform, 55 %, R_f value (F_{256}silica gel) iodine vapour.0.58 (CH_3OH/NH_3 /$C_4H_9O_6$ 0.8:2.0:5.2). IR (KBr)ν_{max} 3476, 1735, 1634, 1556, 1462, 1352, 1323, 1155, 1037, 976. ^{1}H-NMR ($CDCl_3$)δ: 1.30–1.03 (m, 4H, CH_2CHCH_2), δ: 3.31 (s, 3H, NH_3 +), δ: 3.71 (m, 1H, CH_2CHCH_2), δ: 3.84 (m, 1H, pyrrolidine CH_2), δ: 3.93 (s, 3H, OCH_3), δ: 4.46 (m, 1H, pyrrolidine CH_2), δ: 4.58 (s, 2H, pyrrolidine CH_2), δ: 6.89-6.155 (m, benzyl ring), δ: 8.60-8.06 (s, 1H, CH). EIMS: m/z (R.A %) 484 [M^{+1}] (0.53), 374 (0.24), 346 (1.24), 300 (1.59), 263 (2.13), 234 (0.91), 219 (28.07), 204 (7.92), 163 (2.52), 110 (25.43), 96 (88.07), 93(2.75), 78 (100) base peak, 78 (96.66).

Synthesis of derivatives G-D09 & G-D10

Synthesis of derivatives G-D09 & G-D10 was achieved by taking equi-molar methanolic solution of drug and reagent (benzoic acid and 2-amino benzoic acid) were mixed having $SOCl_2$, followed by refluxing at 90^{o}C by nucleophilic substitution as mentioned in scheme 1. The carboxylic acid group of reagents first reacts with sulfonylchloride ($SOCl_2$) an acyl halide to form acid chloride which is reactive species, coupled with the amino group of GMFX to give amide.

(Z)-7-(3-(benzamidomethyl)-4-(methoxyimino) pyrrolidin-1-yl)-1-cyclopropyl-6-fluoro-4-hydroxy-1, 4-dihydro-1, 8-naphthyridine-3-carboxylic acid (G-D09)

493.05, 190°C, Brown, DMSO, methanol, Chloroform, 81%, R_f value (F_{256}silica gel) iodine vapour.0.76 (CH_3OH/NH_3 /$C_4H_9O_6$ 0.8:2.0:5.2), FT-IR (KBr)ν_{max}3373, 3174, 2927, 1743, 1656, 1566, 1508, 1394, 1186, 945. ^{1}H-NMR ($CDCl_3$) δ: 1.30–1.03 (m, 4H, CH_2CHCH_2), δ: 3.25 (s, 3H, NH_3 +), δ: 3.61 (m, 1H, CH_2CHCH_2), δ: 3.84 (m, 1H, pyrrolidine CH_2), δ: 3.93 (s, 3H, OCH_3), δ: 4.46 (m, 1H, pyrrolidine CH_2), δ: 4.58 (s, 2H, pyrrolidine CH_2), 7.18-7.83 (m, benzyl ring), 6.72-6.53(d, 1H, J = 0.030, amide), δ: 4.36-4.37 (m, 1H, pyrrolidine CH_2). EIMS: m/z (rel. abd %) 494 [M^{+1}] (0.56), 390 (0.91), 345 (1.54), 316 (2.10), 273 (2.23), 204 (1.19), 164 (3.11), 105 (86.92), 96 (4.72), 79 (9.13), 77 (100) base peak.

(Z)-7-(3-((3-aminobenzamido) methyl)-4-(methoxyimino) pyrrolidin-1-yl)-1-cyclopropyl-6-fluoro-4-hydroxy-1,4-dihydro-1,8-naphthyridine-3-carboxylic acids (G-D10)

508.52, 110°C, Light browns, DMSO, methanol, Chloroform, 60%, R_f value (F_{256}silica gel) iodine vapour 0.69 (CH_3OH/NH_3 /C_4H_9O6 0.8:2.0:5.2), FT-IR(KBr)$\nu_{max,}$ 3454, 2947, 1745, 1653, 1562, 1465, 1209, 1045,912. ^{1}H-

NMR ($CDCl_3$) δ: 1.30–1.03 (m, 4H, CH_2CHCH_2), δ: 3.21 (s, 3H, NH_3 +), δ: 3.59 (m, 1H, CH_2CHCH_2), δ: 3.84 (m, 1H, pyrrolidine CH_2), δ: 3.93 (s, 3H, OCH_3), δ: 4.46 (m, 1H, pyrrolidine CH_2), δ: 4.58 (s, 2H, pyrrolidine CH_2), 7.32-7.95 (m, benzyl ring), δ: 6.66-6.46(d, 1H, J = 0.026, amide), δ: 4.36-4.37 (m, 1H, pyrrolidine CH_2). EIMS: m/z (rel. abd %) 509 [M+1] (0.32), 390 (0.85), 345 (1.34), 316 (1.18), 273 (6.34), 204 (2.13), 164 (1.21), 119 (100) base peak, 96 (12.77), 91 (82.97), 79 (10.90), 78 (12.61).

In-silico ADMET Analysis

Prediction of pharmacokinetics (ADME) and drug-like properties of candidate compounds is crucial to minimize drug recall at Phase IV of clinical trials. Swiss ADME, Pre-ADMET web-based applications, and T.E.S.T (Toxicity Estimation Software Tool) (U.S. EPA, 2020). employed to predict *in-silico* molecular descriptors, pharmacokinetics, toxicity, and drug-like properties of studied molecules whereas, BioTranformer 3.0 online tool used to predict metabolism of the compounds. (Shamim, Naseem *et al*., 2024; Mun, Bhin *et al.,* 2019; CCTE, EPA 2022)

DFT parameter Studies

The synthesized structures were optimized to their minimum energy states using the B3LYP functional in combination with the 6-311++ (d,p), a triple ζ basis set. These calculations were applied on Gaussian software package, which was chosen for its precision and computational efficiency. (CCTE, EPA 2022) for determining highest occupied molecular orbital (HOMO) and lowest unoccupied molecular orbital (LUMO), same combination of the B3LYP functional and 6-311++ (d, p) basis set was employed. Only structures that exhibited zero imaginary frequencies after optimization and considered for further analysis. For visualization generated Frontier Molecular Orbital (FMO) surface map, using Gauss view software. This allowed for graphical representation of HOMO and LUMO orbitals, interpreting the electrical properties of molecules. The supporting information contains the molecular coordinates for reference.

Microbiological screening

Disc diffusion method, applied for microbial responsiveness of analogues, using GMFX as internal standard against selected organisms (Gram +ve, and Gram –ve). Organisms supplied for study by Dr. Essa Laboratory and Diagnostics (Pvt.) Ltd are ATCC coded *Bacillus subtilus* (6051-U), *Micrococcus luteus* (10786), *Staphylococcus aureus* (29213), S*chizosaccharomyces features* (24843), *Salmonella typhi* (2881), *Proteus mirabilis* (29906), *Pseudomonas aeruginosa* (27853), Escherichia coli (25922), *Shigella flexneri* (29903), *Klesbellia pneumonia* (43816), *Candida albicans* (3147) and *Citrobacter freundii* (13316). (Medimagh M *et al*., 2023)

For this, antibacterial and control discs (3mm) were prepared by soaking analogues solution (0.1%DMSO) of three concentrations (5, 10, and 20 $\mu g\ mL^{-1}$), using Muller–Hinton agar, inoculated with organisms (n=3) (Begum *et al*., 2022) in comparative manner with 0.50 McFarland standard (1.0 × 108 CFU per mL) bacterial strains. Antifungal profiling achieved on same concentrations, using Sabrouse dextrose (SDS) media. Digimatic calipers, (Mitutoyo Rochester, New York, NY, USA) was used for precise measure of zone of inhibitions (ZI, n=3).

STATISTICAL ANALYSIS

SPSS version 22.0 was used for One-way ANOVA and post-hoc analysis (95% CI) using mean value ± standard deviations as input data for variances calculations. (Shamim, Naseem *et al*., 2022)

Molecular Docking studies

Parent molecule (GMFX) and its derivatives (G-D08- G-D10) structures were designed by using Chem Draw Ultra 8.0 (Windows Operating) software. These structures were imported to Molecular Operating Environment (MOE 2018.01, Chemical Computing Group. Inc., Canada) software for adding hydrogen atoms, partial charges (MMF94 modified) and energy minimization (MMFF94x force field). The crystallographic 3D structure of 6K63 (*Klebsiella Pneumoniae*) (liu, Shang *et al*., 2019) 1AI9 (*Candida albicans*) (Atef, Al Farraj *et al*., 2020) and 3JWB (*Citroacter ferundii*) (Kaddouri, Bouchal *et al.,* 2021) were retrieved, from online free server RCSB Protein Data Bank (http://www.rcsb.org/pdb). Protein chains were refined and used only monomers, added to MOE for removal of water molecules, heteroatoms, addition of hydrogen atom/s, missing residues, partial charges (MMF94 modified), and energy minimization (MMFF94x force field). For active sites prediction MOE alpha site finder was used, molecular docking studies through MOE were performed via default parameters i.e., placement and refinement method (Triangle Matcher + Induced fit) and scoring function (London dG + GBVI/WSA dG). For each synthesized scaffold, conformations (n=5) were allowed to be formed. Top-ranked conformations with a root mean square deviation (RMSD) less than 2°A were selected. Their 2D and 3D poses were generated and saved in .png format by using MOE Software and an online source i.e. PLIP (https://projects.biotec.tu-dresden.de/plip-web/plip/index). The interactions are elaborated in different binding forms like Hydrogen bonding (green line), pi-pi/pi-CH stacking, pi-cation, salt bridge and hydrophobic interactions. The parent is represented in a pink tea colour and derivatives in cyano colour in 3D figs. All hydrogen bonds distances were less than and equal to 3°A.

RESULTS

In this work, C-3 modified GMFX ester derivative (G-D08) synthesized by Fischer esterification. Sulphuric acid (conc.) involved in carboxyl carbon protonation thus creates carbocation, leaving water molecules. The oxonium ion lost a proton ester generation, after reacting with hydrogen sulphate ion confirming acid-catalyzed

esterification (Scheme 1). (Zaharani, Khaligh L *et al*., 2021)

The derivatives G-D09 and G-D10 proceeds amide reaction after attacking nitrogen lone pair in GMFX, facilitating nucleophilic reaction, involving carboxylic group of reagent. (Shamim, Naseem S *et al*., 2024) as reflected in scheme 1.

Spectral Studies

The spectral analysis was done in comparative manner with respect to parent molecule gemifloxacin as standard. FT-IR spectra of synthesized derivatives were evaluated carefully, reporting gemifloxacin (parent molecule) broad peak ranges. 3500-3100 cm^{-1} indicates O-H stretching vibrations because of piperizinyl NH, while 3476 cm^{-1} reflects carboxylic acid. (Luo, Lv *et al*., 2020). Attributed peaks of carbonyl stretch υ (C=O) and C=O appear at 1718 cm^{-1} and 1323 cm^{-1}, (Atef, Al Farraj *et al*., 2020). respectively. The changes in derivatives were observed with respect to these main peaks. FT-IR spectra of C-3 modified derivative G-D08 exhibits strong peak at 1735 cm^{-1} indicating the formation of ester linkage which was further assured by absence of peaks at 3509 cm-1 assigned for OH group of COOH while, peak at 3476 assigned for NH group was found undisturbed. Peaks at 1718 cm^{-1} were assigned for C=O (carbonyl) group in GMFX. Spectra of derivatives G-D09 and G-D10 removal of NH peak at 3454-3373 cm^{-1} proved that the NH group of GMFX was involved in derivative synthesis with acyl-chloride. Appearance of new peaks at 1656-1653 cm^{-1}, confirms the formations of amide between –NH group of GMFX and COOH of reagent. These proved the synthesis of the amide band between amine of drug and acyl group of reagents.

To support these changes, H^1NMR spectra were analyzed, with respect to parent molecule (GMFX), exhibiting CH of pyridine peaks at d δ: 8.66 (s, 1H, CH) and δ: 8.01-8.04 (d, 1H). Protonic signals of pyrrolidine ring at δ: 3.84 (m, 1H, pyrrolidine CH_2), δ: 4.58 (s, 2H, pyrrolidine CH_2), δ: 3.93 (s, 3H, OCH_3), δ: 3.71 (m, 1H, CH_2CHCH_2), δ: 4.46 100 (m, 1H, pyrrolidine CH_2), δ: 3.42 (m, 101 1H, pyrrolidine CH). Signals at δ: 3.39–3.21 (m, 2H, pyrrolidine CH_2), and δ: 3.31 (s, 3H, NH_3^+) corresponds to NH_2, while signals at δ: 2.73 (s, 3H, SO_3CH_3) refers to mesylate protons along with peaks at 103 δ: 1.30–1.03 (m, 4H, CH_2CHCH_2) ppm confirming presence of 1 beta N-cyclopropyl in drug structure.

Spectra of derivative G-D08, showed absence of signals at 11 ppm confirming involvement of GMFX carboxylic group in reaction, assured by appearance of signals at δ: 6.89-6.155 (aromatic ring presence), and peaks shifting to δ:8.60-8.06 ppm (s, ^{1}H, CH of pyridine) while other peaks remain unchanged. ^{1}HNMR spectra of synthesized derivatives (G-D09 and G-D10), showed a new singlet peak at δ: 6.72-6.46 ppm representative of C-NH amide bond authenticated by appearance of peaks at δ: 7.18-7.95 ppm, assigned for aromatic rings, newly attached.

In-silico ADME parameters studies

Molecular descriptors of all three compounds demonstrated excellent physicochemical properties (table 1) except G-D10 which has a slightly higher molecular weight, due to which it violates Lipinski's rule of five. The molar refractivity (MR) of the compounds is also closer to the ideal range (40-130) of drug-like compounds. Drugs exhibiting octanol/water partition coefficient (Log Po/w) value below zero (injectable), 0-3 (oral administration), 3-4 (transdermal patches), while higher values represents toxicity in fatty tissues (Kaddouri, Bouchal *et al*., 2021) Our compounds represented Log Po/w in the range of 1.9-2.7 which indicates oral absorptivity of the compounds. The percentage of human intestinal absorption of all three compounds is above 90% indicates that compounds have greater gastrointestinal absorption (Singh, Khan *et al*., 2023).

P-Glycoprotein (P-gp) is a common carrier in drug intestinal penetration. The compounds under investigation are P-gp substrate means that they are easily absorbed through the intestine. Skin permeation coefficient (LogKp) is the measure of the conduction of compounds through the skin. A negative LogKp value indicates good skin absorption. According to one classification blood-brain barrier (BBB value) less than 0.1 represents that compounds show very low absorption to CNS and cannot cross blood-brain barrier so CNS-inactive. (Geldenhuys, Mohammad *et al*., 2015). PCaco-2 value of almost 20 nm/sec indicates intermediate cell permeability of compounds (Wu, Zhou *et al*., (2020). The quantity of drug bound to the plasma protein determines the availability of the drug to the target. Only the amount of unbound drug is available for diffusion across cell membranes and binding to the target. The percentage of Plasma protein binding (% PPB) less than 70% is an indication of weak interaction of the compounds with plasma proteins, providing good bioavailability, as given in the table 2. Cytochromes help in the metabolism of compounds. The compounds, which are inhibitors of cytochromes, exhibits poor metabolism. G-D08 is a non-inhibitor of Cyp2C19, Cyp2D6, and Cyp3A4, whereas compounds G-D09 and G-D10 are inhibitors of Cyp3A4. However, all three compounds are non-inhibitors of most of the cytochromes, indicative of effective metabolism. According to BioTransoformer version 3.0, during phase II metabolism inside humans, G-D08 undergoes aromatic OH-Glucuronidation by UDP-glucuronosyltransferase and sulfation of secondary alcohol by Alcohol sulfotransferase, G-D09 undergoes O-Glucuronidation of aliphatic acid and glycine conjugation through Glycine N Acyltransferase whereas in G-D10, glucuronidation of primary aromatic amine also occur along with glucuronidation of aliphatic acid and glycine conjugation. Toxicity prediction suggests that the compounds are non-mutagenic, with slight toxicity. According to the Hodge-and-sternal scale the oral rat LD50 within a range of 500-5000 mg/kg are slightly toxic. (CCTE, EPA 2022).

Table 1: Physicochemical and Computational structural details of derivatives

Compounds	G-D08	G-D09	G-D10
Formula	$C_{24}H_{26}FN_5O_5$	$C_{25}H_{26}FN_5O_5$	$C_{25}H_{27}FN_6O_5$
Molecular weight	483.49	493.05	508.52
M.P °C	154°C	190°C	110°C
Color	Brown	Brown	Light browns
Solubility	DMSO, methanol, Chloroform	DMSO, methanol, Chloroform	DMSO, methanol, Chloroform
Yield (%)	55	81	60
Iteration	198	1.61	258
Stretch	1.887	16.52	1.52
Bend	18.94		17.76
Torsion	0.25	4.34	1.5
Non-1,4 VDW	-6.78	-5.67	-7.94
1,4 VDW	20.33	20.58	20.26
Stretch-band	0.04	0.12	0.13
Dipole-Dipole	2.35	-3.44	-3.66
Total energy	37.04	34.06	29.59
UV nm (e)	293	292	289

Table 2: *In-silico* ADME parameters of the derivatives

Parameters		G-D08	G-D09	G-D10	Prediction Tools
Molecular Descriptors	MW (g/mol)	483.5	493.5	508.5	
	Heavy Atoms	35	36	37	
	Rotatable bonds	7	8	8	
	HBD	3	2	3	
	HBA	9	8	8	SwissADME
	Molar Refractivity	131.96	133.03	137.43	
	TPSA (Å)	133.74	126.12	152.14	
Pharmaco-kinetics (ADME)	$LogP_{o/w}$	1.93	2.70	2.51	
	Buffer solubility (mg/L)	(2.22) Soluble	(17.17) Soluble	(13.05) Soluble	PreADMET
	%HIA (GI Absorption)	(92.15) High	(96.64) High	(90.95) High	
	BB (C_{brain}/C_{blood})	0.031	0.061	0.047	
	P_{Caco-2} (nm/sec)	20.1	20.3	20.0	
	%PPB	60.73	84.73	63.34	
	$LogK_p$ (cm/s)	-7.62	-6.83	-7.40	
	P-gp Substrate	Yes	Yes	Yes	SwissADME
	Cyp2C19 Inhibitor	No	No	No	
	Cyp2D6 Inhibitor	No	No	No	
	Cyp3A4 Inhibitor	No	Yes	Yes	
	Phase II Metabolism	Ar OH-glucuronidation & Sulfation of sec.alcohol	Glucuronidation of acid & Glycine conjugation	Glucuronidation of acid & prim.amine, & Glycine conjugation	BioTransformer
Toxicity	Oral Rat LD50 (mg/Kg)	2406.53	1368.74	753.21	TEST software
	Mutagenicity	(0.28) Negative	(0.50) Negative	(0.35) Negative	
	Fathead Minnow LC50 (mg/L)	0.019	0.012	0.012	
	Ames Test	Mutagen	Mutagen	Mutagen	
	hERG Inhibitor	High risk	Medium risk	High risk	
Drug likeness	Lipinski's Rule	Suitable	Suitable	1 Violation	PreADMET
	Lead-like Rule	1 Violation (MW>350)	1 Violation (MW>350)	1 Violation (MW>350)	

Table 3: Interactions of compounds G-D08, G-D09 and G-D10 with *Klebsiella Pneumoniae* (6K63), *Citrobacter ferundii* (3JWB) and *Candida albicans* (1AI9)

Interactions of compounds G-D08, G-D09 and G-D10 with *Klebsiella Pneumoniae* (6K63)						
Compounds	Binding Energy (kcal/mol)	Hydrogen bonding (3°A)	Pi-pi/pi-CH	Pi-cation	Salt bridge	Hydrophobic interactions
G-D08	-7.7996	Thr100, His102, His131, Asn234			His102, His131	Met97, Gln98, Asn234, Leu270
G-D09	-7.4761	His102	Gln98			Glu91, Gln98, Thr100, Asn234
G-D10	-7.6622	Gln98, His105	/Gln98			Thr96, Gln98, Gln99, Ala275
Gemifloxacin	-5.8973	His131, Gln272				
Interactions of compounds G-D08, G-D09 and G-D10 with *Citrobacter ferundii* (3JWB)						
Compounds	Binding Energy (kcal/mol)	Hydrogen bonding	Pi-pi/pi-CH	Pi-cation	Salt bridge	Hydrophobic interactions
G-D08	-6.6424	His335, Val338, Arg375	/Val338, Ile388		Arg374	Ala366
G-D09	-7.2115	His117, His335,	His117 (P)		His117	Tyr113, Thr354, Ala366
G-D10	-6.0526	Tyr113, His355, Arg374	Tyr113 (T), His117 (P)			Tyr113, Ala366, Ile368
Gemifloxacin	-4.5811	His355, Arg374			Arg374	Phe188, Leu340
Interactions of compounds G-D08, G-D09 and G-D10 with *Candida albicans* (1AI9)						
Compounds	Binding Energy (kcal/mol)	Hydrogen bonding	Pi-pi/pi-CH	Pi-cation	Salt bridge	Hydrophobic interactions
G-D08	-5.3938	Ala11, Gly23, Glu32, Thr58				Ile19, Phe36, Lys57, Thr58, Tyr118
G-D09	-6.5034	Ala115	Phe36 (P) /Lys57	Lys57		Phe36, Lys57, Thr58, Glu116
G-D10	-7.4879	Ala11, Lys22, Thr58	Phe36 (P) /Gly23			Ile33, Phe36, Ile62
Gemifloxacin	-5.9282	Ala11, Ser61, Tyr118	/Phe36			Lys24, Phe36

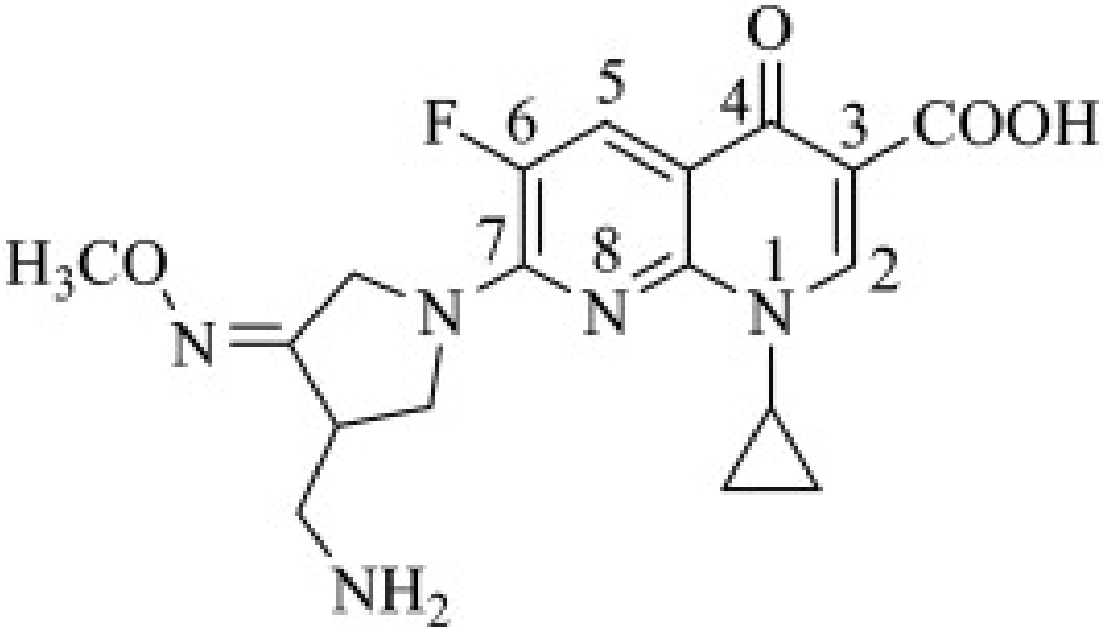

Fig. 1: Gemifloxacin

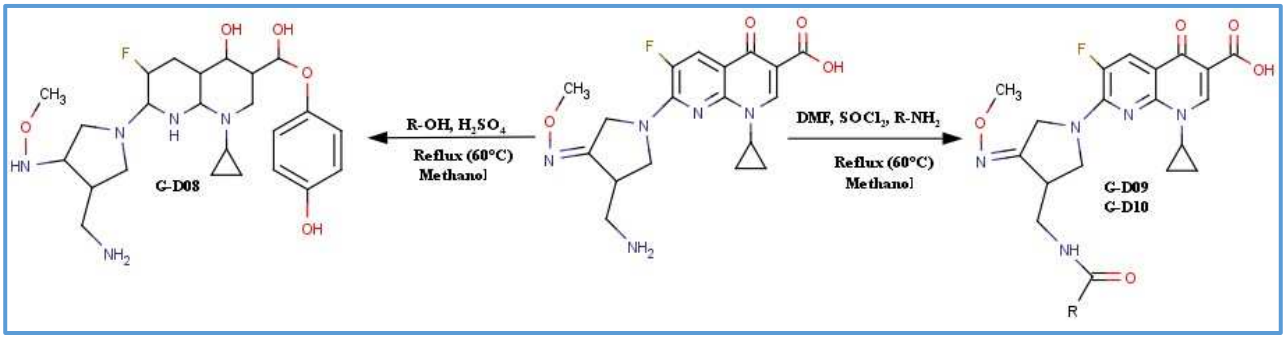

Scheme 1: Synthesis of G-D08, G-D09, and G-D10.

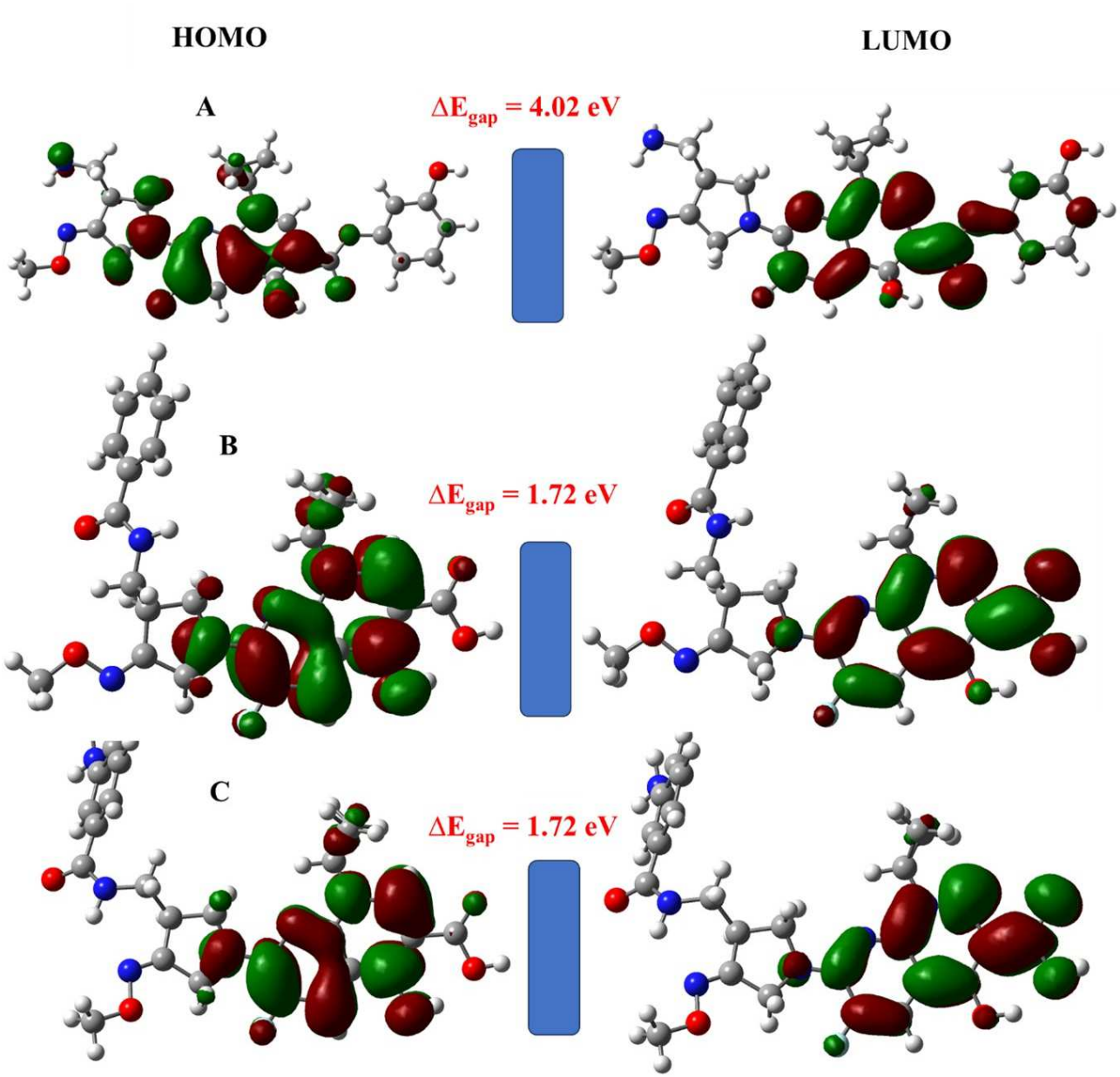

Fig. 2: HOMO and LUMO with HOMO-LUMO gap.

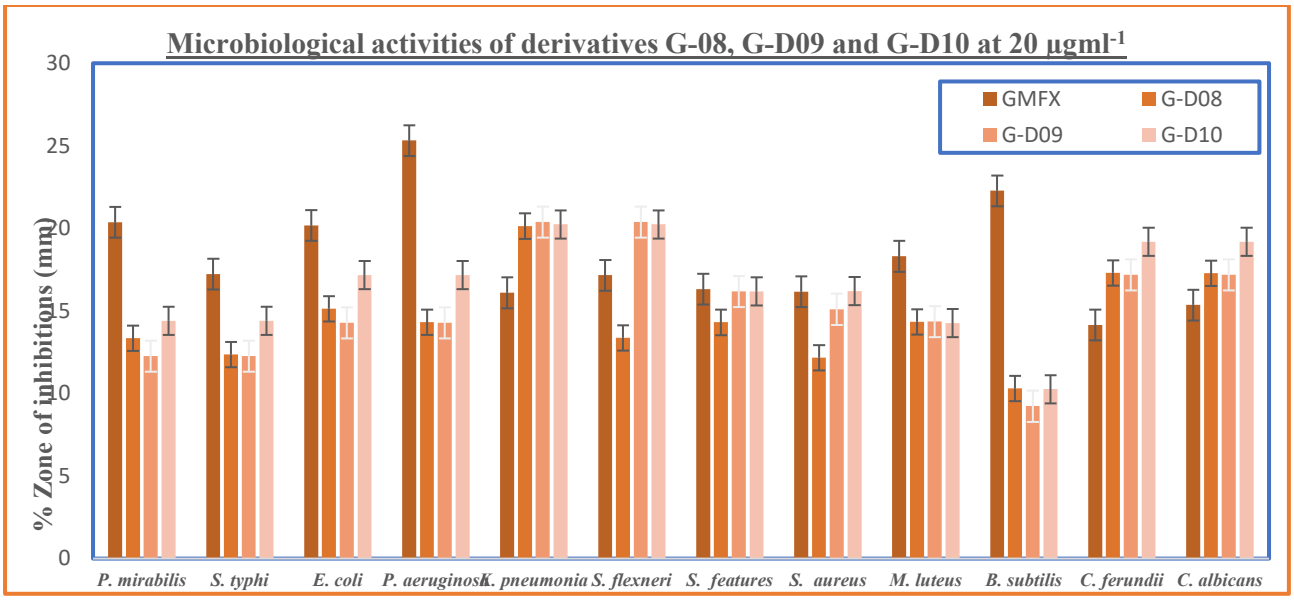

Fig. 3: *In-vitro* microbiological activities of derivatives against the selected gram positive, gram negatives and fungal species.

Analysis of HOMO and LUMO

In chemistry and quantum mechanics, HOMO and LUMO are important concepts used to investigate electronic structure of molecules and their reactivity. (Pir, Günay *et al*., 2012) These orbitals play a significant role in understanding various chemical phenomena, including bonding, stability, and chemical reactions. The HOMO is crucial because it determines molecule's chemical and physical properties related to electron donation or ionization, primarily involved in chemical reactions through ionization potential (IP). The energy difference between HOMOs of two interacting molecules can influence ease of electron transfer between them; generally, more spatially extended compared to lower energy orbitals. (Miar, Shiroudi *et al*., 2021)

On the other hand, LUMO represents lowest energy molecular orbital that does not contain any electrons. It is the first vacant orbital above the HOMO and is involved in accepting electrons during chemical reactions. The LUMO is crucial in understanding electron acceptance, such as in nucleophilic attack or electron transfer processes. (Singh, Khan *et al.,* 2023) In this study, we conducted an analysis to map the iso-surfaces of HOMO and LUMO, as well as the gap of HOMO-LUMO.

Fig. 2 illustrates shapes of HOMO and LUMO orbitals. We observed that HOMO is predominantly distributed over nitrogen atom-containing rings, suggesting that electron donation interactions occur from nitrogen-containing regions of these molecules. Conversely, empty orbitals or HOMO, mainly localized around oxygen-containing regions of derivatives. This portion of derivatives acts as an electrophile, facilitating electron acceptance interactions. Consequently, any electron gaining interactions would predominantly occur in this area. Derivatives G-D09 and G-D10 exhibit only slight structural differences, leading to similar HOMO and LUMO structures and, consequently, similar chemical properties. These derivatives can be classified as aromatic due to delocalization of HOMO and LUMO orbitals. In aromatic compounds, HOMO and LUMO orbitals often exhibit characteristic delocalization and symmetry, contributing to molecule's stability and unique properties.

Microbiological screening

As per WHO report 2019, drug resistance is main causative factor for death of 7 million people around the globe. Among which 44.2 % was affected by *Escherichia coli*, 20.6 % by, *S. aureus*, 11.3% by *K. pneumoniae* and 5.6% by *Pseudomonas aeruginosa* along with other organisms like 5.3% *E. faecium* and 4.5% *Acinetobacter spp*. Another study conducted by WHO's latest Global Antimicrobial Surveillance System (GLASS) 2020 suggested involvement of *E. coli*, *S. aureus*, *S. pneumoniae*, and *K. pneumoniae* as most widely identified resistant bacteria. (Uddin, Chakraborty *et al*., 2021). Therefore, in light of these studies, organisms were selected for studies.

The Gemifloxacin derivatives were evaluated towards antimicrobials against selected Gram-negatives, Gram-positives, and fungi by disc diffusion method at three different concentrations of derivatives (5, 10, and 20 μgmL^{-1}), statistical analysis (student's t-test) was carried out to analyze variations among inhibitory zones of all synthesized derivatives at $p \leq 0.05$ as significant (fig. 3).

Molecular Docking studies

Synthesized Derivatives with 6k63

Gly94, Ala95, Gln98, Thr100, His102, Tyr126, Tyr127, Gly130, His131, Arg133, Gln134, Arg152, Tyr160,

Pro162, Asp163, Asp169, Asn234, Pro269, Ile271, residues were consider in catalytic pocket of 6K63 and among them fourteen residues (Gly94, Ala95, Gln98, Thr100, Gly130, His131, Arg133, Gln134, Pro162, Asp163, Ala200, Asn234, Thr263 and Ile271) participated in hydrogen bonding or salt bridges formation (Wie liu 2019). All derivatives along with the parent molecule very well fixed in the catalytic pocket of 6K63 but G-D08 showed highest binding affinity towards active site in term of least score by sharing its carboxylate OH, phenol OH and quaternary amine via five hydrogen bonds and salt bridge (table 3: fig. 4).

It shows that addition of phenol ring at carboxylic site increases potential of drug and makes it more potent. G-D09 formed only one hydrogen bond with His102 and pi-CH with Gln98 showed that when benzoyl was introduced at amine position, activity of derivative slightly dropped. On the other hand, the substituted benzoyl moiety at similar position makes G-D10 molecule with better score as compared to G-D09 by forming two hydrogen bonds with Gln98 and His102 along with pi-CH interaction (Gln98) but Gemifloxacin only interact with active side via two hydrogen bonds i.e. His131 and Gln272.

The orientation of molecules in pocket is very important. G-D08 and G-D10 had attained standard position i.e. facing its carboxylate group towards His131 with good binding scores while G-D09 entered in active pocket with rotation from other two derivatives with less score (better than parent), its carboxylate towards Thr236 amino acid. Hydrophobic zone for all derivatives was included Glu91, Thr96, Met97, Gln98, Gln99, Thr100, Asn234, Leu270, Ala275 residues.

Synthesized Derivatives with 3jwb

Published works demonstrated that some of amino acids located in binding pocket of 3jwb are essential for catalytic reaction such as cysteine (Cys) and arginine (Arg), which can lead to the inhibition of the bacteria (Kaddouri, Bouchal *et al.,* 2021). The essential residues of catalytic triad (Ser39, Tyr113, Asn160, and Arg374) played a significant role in clamping ligands by forming hydrogen bonds.

The amino acids of a hydrophobic pocket formed by side groups of the residues of both monomers of the catalytic dimer are Tyr113, Cys115, Ala118, Phe188, Thr209, Val338, and Leu340 of the first monomer and Phe49, Leu57, Tyr58, Leu61, and Phe235 of the second monomer. (Anufrieva, Morozova *et al*., 2015). Compounds G-D08, G-D09, G-D10 and parent were docked with the active site to generate their binding mode. G-D10 was bind to receptor residues via five possible hydrogen bonds with Tyr113, His355 and Arg374 amino acids with distances of less or equal to 3˚A along with pi-pi interaction with Tyr113 and His117and three Van der Waal interactions with Tyr113, Ala366 and Ile368 residues.

However, the study reveals that compound G-D08 formed three hydrogen bonds with His335, Val33 and Arg374, two pi-CH stacking with Val338 & Ile368 and only one salt bridge with Arg374 residue and one hydrophobic interaction with Ala336. (table 3) Another compound G-D09 also showed the two hydrogen bond interactions from His117 & His335, hydrophobic contact of Tyr113, Thr354, Ala366, π–π interaction between the aromatic rings of compound and His117 and salt bridge between carboxylate and His117. (fig. 5) Parent compound Gemifloxacin interacted via 3 hydrogen bonds with His355 and Arg374 along with one salt bridge (Arg374) and 2 hydrophobic interactions (Phe188, Leu340).

The maximum interaction was shown by G-D10 compound, G-D10 contained amino substituted benzoyl ring, and this attachment changed the binding orientation of the compound as compare other derivatives and parent.

Synthesized Derivatives with 1AI9

According to reported work, Candida albicans dihydrofolate reductase (1AI9) are the main target for antifungal drugs. The active site residues of 1AI9 include Arg56, Lys57, Ser78, Ala111, Ile112, Gly114, Tyr118 are important for hydrogen bonding, whereas residues Ile9, Ala11, Met25, Ile33, Phe36, Lys37, Ile62, Leu69, Ile112 and Tyr118 were involved in hydrophobic interactions. (Nadaf, Najare *et al*., 2020; Atef, Al Farraj *et al*., 2020).

The compounds studied have shown good docking scores against the enzyme dihydrofolate reductase of Candida albicans as revealed by the docking study. (table 3) fig. 6 represents the docked view of G-D08, G-D09, G-D10 and Gemifloxacin in the active pocket of the enzyme PDB ID: 1AI9.

All compounds are fixed in the active pocket but interacting with different residues. Gemifloxacin (parent) showed five H-bonds with three different residues including Ala11, Ser61 and Tyr118. G-D08 showed four Hydrogen bonds with Ala11, Gly23, Glu32 and Thr58 of 1AI9. G-D09 made only one Hydrogen bond (Ala115), pi-pi (Phe3), pi-CH (Lys57) and pi-cation (Lys57). Compound G-D10 also formed three Hydrogen bonds (Ala11, Thr58 and Lys22) along with pi-pi and pi-CH (Phe36 and Gly23 respectively) interactions.

The all synthesized molecules showed hydrophobic interactions with reported amino acids (table 3). Compound G-D09 and G-D10 interacts at active site in same manner as they possess similar substitutions unlike compound G-D08 in which attachment at carboxylate which rotates whole molecule in active cavity. All synthesized compounds are bulky showed a well fit sketch of binding in catalytic site and with catalytic residues adopt most favorable and greater interactions among which G-D10 have maximum number of interactions.

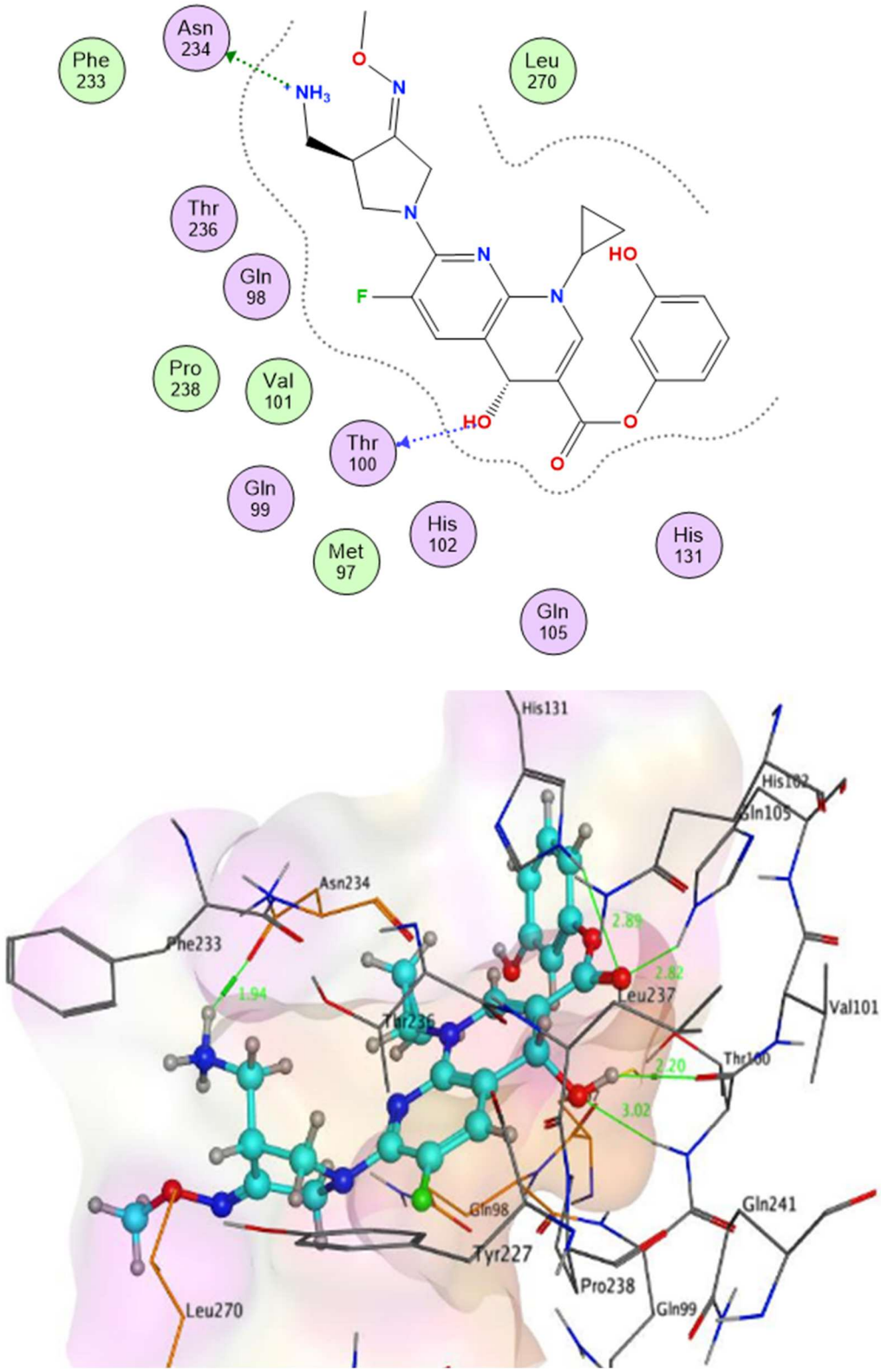

Fig. 4: 2D and 3D pic of G-D08 with 6k63

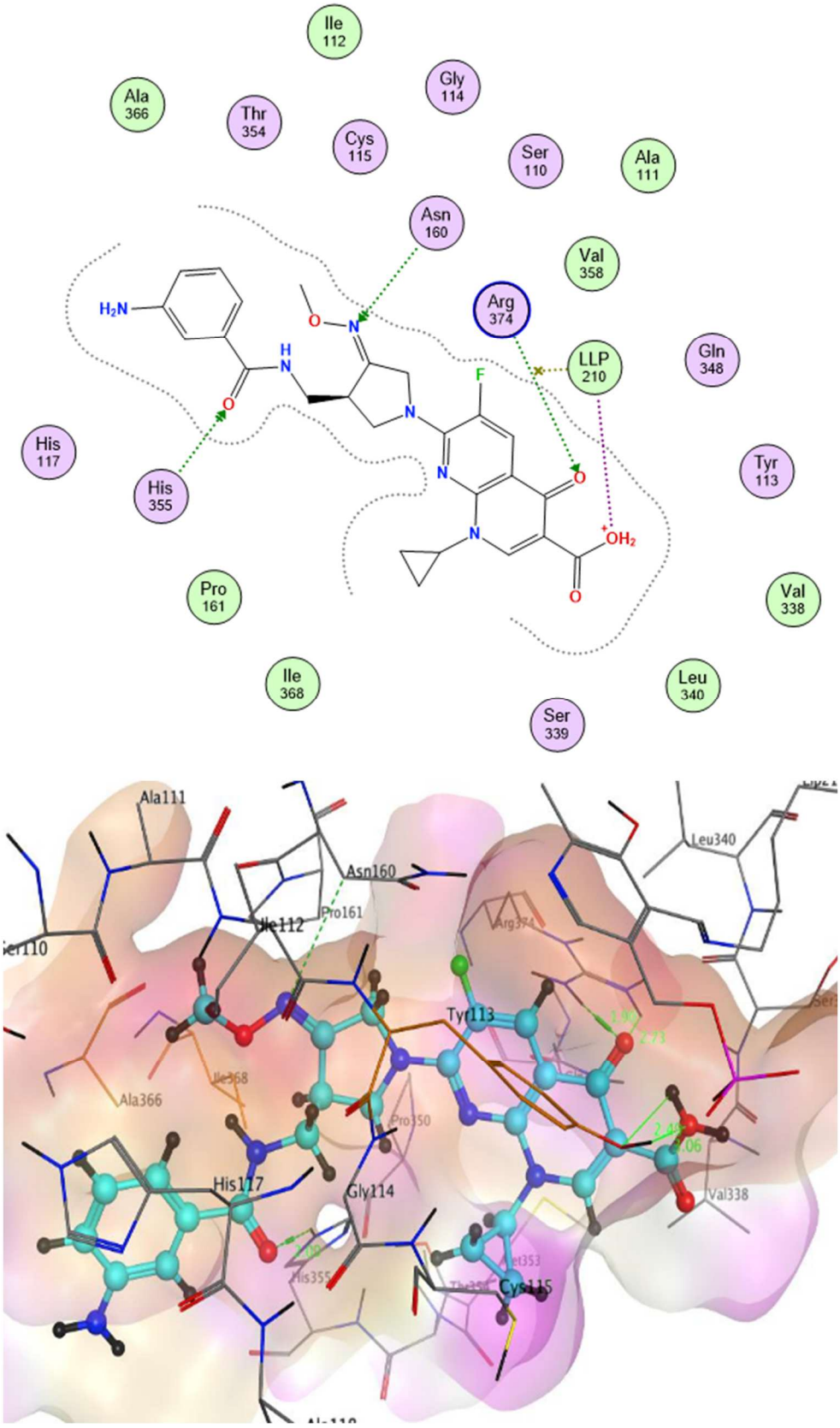

Fig. 5: 2D and 3D pic of G-D10 with 3JWB

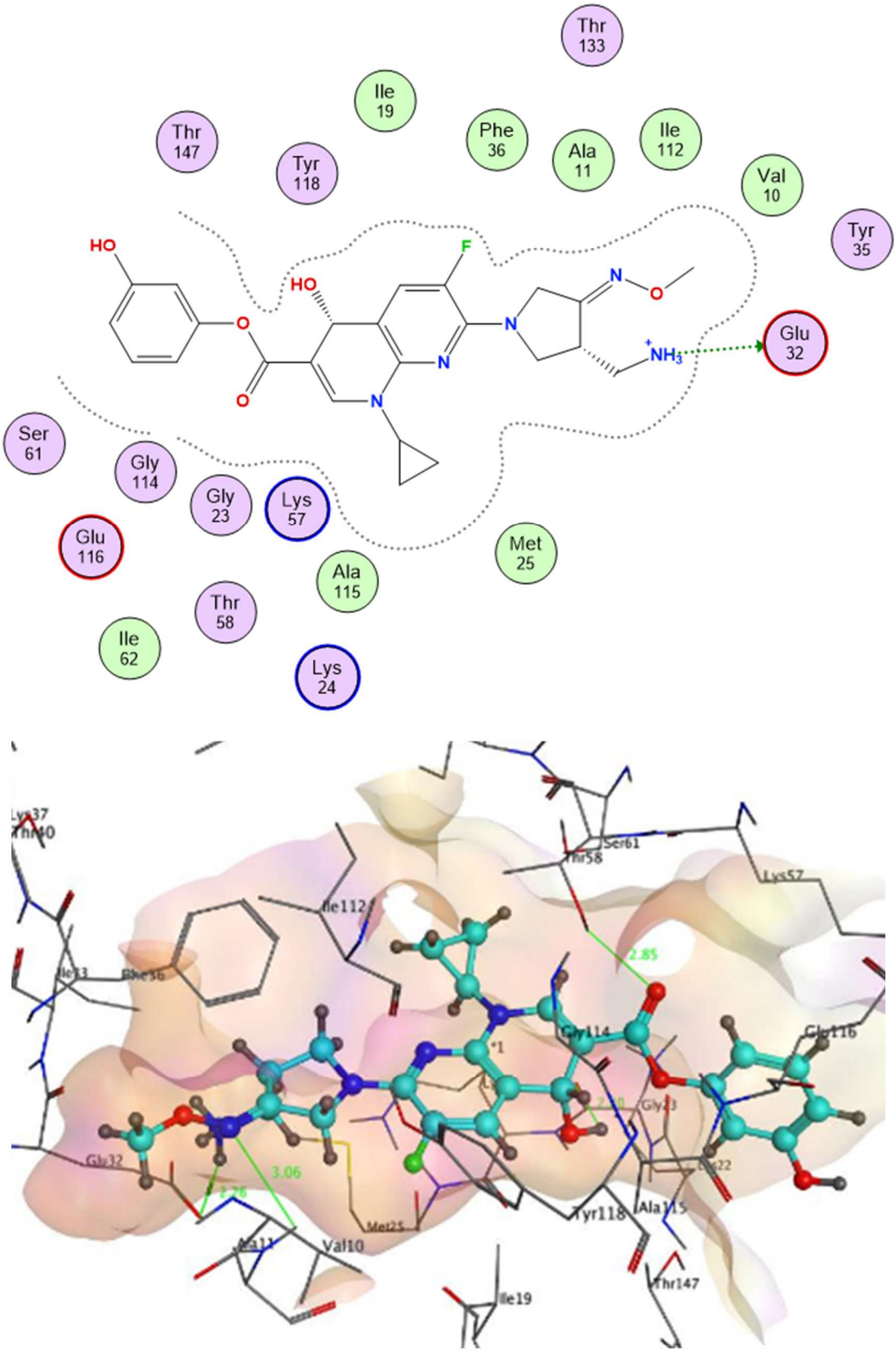

Fig. 6: 2D and 3D pic of G-D08 with 1AI9

DISCUSSION

Derivatives, G-D08 (C-3 modified), G-D09 and G-D10 (C-7 modified) synthesis was achieved via C-3 Fischer esterification, (Zaharani, Khaligh *et al*., 2017) and nucleophilic reaction, involving carboxylic group of reagent, respectively as shown in (Scheme 1). Spectral comparative approach applied to affirm their synthesis by FT-IR, NMR and Mass spectroscopy. Firstly, FT-IR spectral reveals that in GMFX spectra, O-H stretching vibrations at 3500-3100 cm^{-1} because of piperizinyl NH, while 3476 cm^{-1} reflects carboxylic acid changes in derivatives observed with attributed peaks. Strong peak at 1735 cm^{-1} indicates esterification in G-D08 and absence of OH group of COOH, exhibiting peaks at 3509 cm-1 with undisturbed NH group peak at 3476. While in G-D09 and G-D10 absence of NH peak at 3454-3373 cm^{-1} reports the involvement of NH group, evident of synthesis. Supported by H^1NMR, where G-D08, have no signal at 11 ppm and G-D09 and G-D10 showed singlet peak at δ: 6.72-6.46 ppm representative of C-NH amide bond.

Toxicity prediction suggests that compounds are non-mutagenic, with slight toxicity. (Rim, 202)). However, possess high risk of hERG. Stability (fig. 2) by DFT studies indicate HOMO-LUMO gap of G-D09 and G-D10 is 1.72 eV and G-D08 is 4.02 eV, over analysis of molecules concludes that G-D09 and G-D10 are more reactive than G-D08. Close HOMO and LUMO energy levels indicates easy acceptance or donation of electrons, making them more reactive as smaller energy gaps are responsible for intra-molecular charge transformation (Miar, Shiroudi *et al.*, 2021).

The data obtained from *in-vitro* microbiological studies of derivatives reveals lesser activity with reference to parent molecule (GMFX), exception is found only against *K. pneumonia* and *C. ferundii* where all compound possess activity higher than parent drug (GMFX).

The antifungal response of synthesized derivatives against *C.albicans* reveals that all three derivatives were active against said specie. (Ashraf, El-Barrawy *et al.,* 2022). Among all the studied compounds, G-D10 was most potent, while G-D09 and G-D08 exhibits lesser antifungal activities but much better in comparison to parent molecule (GMFX). Therefore, here we can report that these derivatives have potential to explore as potent antifungal agents (Uddin, Chakraborty *et al*., 2021).

Molecular docking studies reveals that all synthesized compounds showed hydrophobic interactions with amino acids, involved in receptor binding (table 3). Compound G-D09 and G-D10 placement in active site are similar because both have substitution at same point unlike compound G-D08 in which attachment at carboxylate which rotate whole molecule in active cavity. (Shamim, Naseem *et al*., 2024; Rim*.,* 2020) (supplementary data files table 1 and fig. 1-3).

All synthesized compounds are bulky showed a well fit sketch of binding in catalytic site and with catalytic residues adopt the most favorable and greater interactions among which G-D10 have maximum number of interactions.

CONCLUSION

Derivatives reported here G-D08 (C-3 ester), G-D09 and G-D10 (C-7 amide) of GMFX were synthesized and characterized by UV, FT-IR, ^{1}H NMR and mass spectroscopy along with *In-silico* studies (ADMET, DFT and Molecular docking) which showed structural stability, character and potential of these derivatives to exhibit drug like response. Their *in-vitro* microbial profile reveals their potential as antimicrobial and antifungals agent in comparison to the parent molecule against *K. pneumonia, C. ferundii,* and *C. albicans,* affirming that changes in functional group at these positions are involved in altered DNA gyrase binding. These results can correlate the fact that by the insertion of either phenyl ring at position 3 via ester formation or aromatic acid via amide formation at position 7 exhibits improved against some organisms but specifically against the fungal species.

Further insight on mechanism of interaction of these synthesized compounds with microbial organisms, studied by molecular docking specifically against *K. pneumonia, C. ferundii,* and *C. albicans.* Which identifies that these compounds were found potent by comparing binding affinities of parent molecule (-4.5811 kcal/mol), to the compounds (-7.7996 to -5.3938 kcal/mol), indicating their potential receptor interaction and involvement of amino acids.

In this light of study, we report these compounds as stable, safe (ADMET) and potential against resistant organisms and fungal agent also, which still needs further exploration and molecular mechanism identification.

ACKNOWLEDGEMENT

The authors acknowledge Higher Education Commission (H.E.C), Pakistan for supporting this work under Indigenous 5000 PhD Programme.

Supplementary data

Supplementary data files contain table 1 and fig. 1-3.

Conflict of interest

All contributing authors declare no conflict of interest.

REFERENCES

Akunuri R, Veerareddy V, Kaul G, Akhir A, Unnissa T, Parupalli R, Madhavi YV, Chopra S and Nanduri S (2021). Synthesis and antibacterial evaluation of (E)-1-(1H-indol-3-yl) ethanone O-benzyl oxime derivatives against MRSA and VRSA strains. *Bioorg. Chem.*, **116**: 105288.

Anufrieva NV, Morozova EA, Kulikova VV, Bazhulina NP, Manukhov IV, Degtev DI, Gnuchikh EY, Rodionov AN, Zavilgelsky GB, and Demidkina TV (2015). Sulfoxides, analogues of L-methionine and L-cysteine as pro-drugs against Gram-positive and Gram-negative bacteria. *Acta Naturae* **7**(**4**): 128-135.

Ashraf HMM, El-Barrawy MA and Omran EA (2022). Garlic-induced proteomic change, anti-biofilm and antifungal susceptibility of *Candida albicans*. *Egyptian Egypt. Acad. J. Biol. Sci., G Microbiol.*, **14**(1): 11-22.

Atef Hatamleh A, Al Farraj D, Salah Al-Saif S, Chidambaram S, Radhakrishnan S and Akbar I (2020). Synthesis, cytotoxic analysis, and molecular docking studies of tetrazole derivatives via N-Mannich base condensation as potential antimicrobials. *Drug Des. Dev. Ther.*, **14:** 4477-4492.

Balogun TA, Omoboyowa DA and Saibu OA (2020). In silico anti-malaria activity of quinolone compounds against *Plasmodium falciparum* dihydrofolate reductase (pfDHFR). *Int. J. Biochem. Res. Rev,* **29**(8): 10-7.

Begum I, Shamim S, Ameen F, Hussain Z, Bhat SA, Qadri T and Hussain M (2022). A combinatorial approach towards antibacterial and antioxidant activity using tartaric acid capped silver nanoparticles. *Processes*, **10**(4): 716.

Dadgostar P (2019). Antimicrobial resistance: Implications and costs. *Infect Drug Resist.,* **12**: 3903-3910.

El-Emam GA, El-Baz AM, Shata A, Shaaban AA, El-Sokkary MM and Motawea A (2023). Formulation and microbiological ancillary studies of gemifloxacin proniosomes for exploiting its role against LPS acute pneumonia model. *J. Drug Deliv. Sci. Technol.,* **81**: 104053.

Ezelarab HA, Abbas SH, Hassan HA and Abuo-Rahma GEDA (2018). Recent updates of fluoroquinolones as antibacterial agents. *Arch. Pharm.*, **351**(9): e1800141.

Fan YL, Wu JB, Cheng XW, Zhang FZ and Feng LS (2018). Fluoroquinolone derivatives and their anti-tubercular activities. *Eur J Med Chem*, **146**: 554-63

Medimagh M, Mleh CB, Issaoui N, Kazachenko AS, Roisnel T, Al-Dossary OM, Marouani H and Bousiakoug LG (2023). DFT and molecular docking study of the effect of a green solvent (water and DMSO) on the structure, MEP, and FMOs of the 1-ethylpiperazine-1, 4-diium bis (hydrogenoxalate) compound. *J. Mol. Liq.*, **369**: 120851.

Hassan HA, Allam AE, Abu-Baih DH, Mohamed MF, Abdelmohsen UR, Shimizu K, Desoukey SY, Hayallah AM, Elrehany MA, Mohamed KM and Kamel MS (2020). Isolation and characterization of novel acetylcholinesterase inhibitors from Ficus benghalensis L. leaves. *RSC Adv.*, **10**(60): 36920-9

Gökalp M, Dede B, Tilki T and Atay ÇK (2020). Triazole based azo molecules as potential antibacterial agents: Synthesis, characterization, DFT, ADME and molecular docking studies. *J. Mol. Struct.,* **1212**: 128140

Jia Y and Zhao L (2021). The antibacterial activity of fluoroquinolone derivatives: An update (2018–2021). *Eur. J. Med. Chem.*, **224**: 113741.

Kaddouri Y, Bouchal B, Abrigach F, El Kodadi M, Bellaoui M, and Touzani R (2021). Synthesis, molecular docking, MEP and SAR analysis, ADME tox predictions, and antimicrobial evaluation of novel mono and tetra alkylated pyrazole and triazole ligands. *J. Chem.*, **2021**(1): 6663245.

Liu W, Shang F, Chen Y, Lan J, Wang L, Chen J, Gao P, Ha NC, Quan C, Nam KH and Xu Y (2019). Biochemical and structural analysis of the Klebsiella pneumoniae cytidine deaminase CDA. *Biochem. Biophys. Res. Commun.*, **519**(2): 280-286.

Luo W, Lv JW, Wang T, Zhang ZY, Guo HY, Song ZY, Wang CJ, Ma J and Chen YP (2020). Synthesis, *in vitro* and *in vivo* biological evaluation of novel graveolinine derivatives as potential anti-Alzheimer agents. *Bioorg. Med. Chem.,* **28**(1): 115190.

Miar M, Shiroudi A, Pourshamsian K, Oliaey AR, and Hatamjafari F (2021). Theoretical investigations on the HOMO–LUMO gap and global reactivity descriptor studies, natural bond orbital, and nucleus-independent chemical shifts analyses of 3-phenylbenzo [d] thiazole-2 (3 H)-imine and its para-substituted derivatives: Solvent and substituent effects. *J. Chem. Res.*, **45**(1-2): 147-158.

Mlynarczyk-Bonikowska B, Kowalewski C, Krolak-Ulinska A and Marusza W (2022). Molecular mechanisms of drug resistance in *Staphylococcus aureus*. *Int. J. Mol. Sci.*, **23**(15), 8088.

Mun DG, Bhin J, Kim S, Kim H, Jung J H, Jung Y, Hwang, D. (2019). Proteogenomic characterization of human early-onset gastric cancer. *Cancer cell*, **35**(1), 111-124.

Geldenhuys WJ, Mohammad AS, Adkins CE, and Lockman PR (2015). Molecular determinants of blood–brain barrier permeation. *Ther. Deliv.*, **6**(8): 961-971.

Nadaf AQA, Najare MS, Garbhagudi M, Mantur S, Sunagar MG, Gaonkar S, Joshi, S and Khazi IAM (2020). Synthesis of 6-[4-(4-propoxyphenyl) piperazin-1-yl]-9h-purine derivatives as antimycobacterial and antifungal agents: *In vitro* evaluation and in silico study. *Chem. Biodivers.*, 17(5): e2000053.

Pir H, Günay N, Avcı D and Atalay Y (2012). Molecular structure, vibrational spectra, NLO and NBO analysis of bis (8-oxy-1-methylquinolinium) hydroiodide. *Spectrochim Acta A Mol Biomol Spectrosc.,* **96**: 916-924.

Rim, KT (2020). In silico prediction of toxicity and its applications for chemicals at work. *Toxicol. Environ. Health Sci.*, **12**(3): 191-202.

Shamim S, Munawar R, Rashid Y, Qadar SMZ, Bushra R, Begum I, Imran M and Quds T (2024). Molecular docking: An Insight from drug discovery to drug repurposing approach, chapter 7. unravelling molecular docking - from theory to practice, Edited by Črtomir Podlipnik, published in London, United Kingdom, 2025 by Intech Open, **27**: 145-178.

Sharma V, Das, R, Mehta DK, Gupta S, Venugopala KN, Mailavaram R and Deb PK (2022). Recent insight into the biological activities and SAR of quinolone derivatives as multifunctional scaffold. *Bioorg. Med. Chem.*, **59**: 116674.

Singh JS, Khan MS and Uddin S (2023). A DFT study of vibrational spectra of 5-chlorouracil with molecular structure, HOMO–LUMO, MEPs/ESPs and thermodynamic properties. *Polym. Bull.*, **80**(3): 3055-3083.

Shamim S, Naseem H, Saeed A, Gul S, Kosar S, Altaf AA and Ameen F (2024). Synthesis, characterization and antibacterial effectiveness of gemifloxacin c-3 modified amide analogs. A theoretical and experimental approach. *J. Mol. Struct.*, **1312**: 138573

Shamim S, Gul S, Rauf A, Rashid U, Khan A, Amin R and Akhtar F (2022). Gemifloxacin-transition metal complexes as therapeutic candidates: Antimicrobial, antifungal, anti-enzymatic, and docking studies of newly synthesized complexes. *Heliyon*, **8**(8): e10378

Sakr ME, El Kafrawy NA, Zewain SK, Refaat SA and Hassanein SA (2022). Long noncoding RNA as a diagnostic tool in vascular complication of diabetes. *Menoufia Med. J.,* **35**(3): 1122.

Stapleton MJ, Ansari AJ and Hai FI (2023). Antibiotic sorption onto microplastics in water: A critical review of the factors, mechanisms and implications. *Water Res.,* **233**: 119790.

Tangwangvivat R, Chaiyawong S, Nonthabenjawan N, Charoenkul K, Janethanakij T, Prakairungnamthip D, Wechtaisong W, Boonyapisitsopa S, Bunpapong N and Amonsin A (2022). The validation of haemagglutinin Inhibition test for the detection of antibodies against canine influenza virus in a guinea pig serum model. *The Thai J Vet Med,* **52**(1): 177-84.

U.S. EPA (2020). User's Guide for T.E.S.T. (version 5.1) (Toxicity Estimation Software Tool): A program to estimate toxicity from molecular structure.

Uddin TM, Chakraborty AJ, Khusro A, Zidan BRM, Mitra S, Emran TB and Koirala N (2021). Antibiotic resistance in microbes: History, mechanisms, therapeutic strategies and future prospects. *J. Infect. Public Health*, **14**(12): 1750-1766.

Wang R, Xu K and Shi W (2019). Quinolone derivatives: Potential anti-HIV agent—development and application. *Arch. Pharm.*, **352**(9): 1900045

Wu F, Zhou Y, Li L, Shen X, Chen G, Wang X, Liang X, Tan M, and Huang Z (2020). Computational approaches in preclinical studies on drug discovery and development. *Front Chem.*, **8**: 726.

Yadav V and Talwar P (2019). Repositioning of fluoroquinolones from antibiotic to anti-cancer agents: An underestimated truth. *Biomed. pharmacother.*, **111**: 934-946.

Zaharani L, Khaligh NG, Johan MR and Gorjian H (2021). Synthesis and characterization of a new acid molten salt and the study of its thermal behavior and catalytic activity in Fischer esterification. *NJC,* **45**(16): 7081-8.

Zhao L, Zhang H, Li N, Chen J, Xu H, Wang Y, and Liang Q (2023). Network pharmacology, a promising approach to reveal the pharmacology mechanism of Chinese medicine formula. *J. Ethnopharmacol.*, **309**: 116306.